GEOPHYSICAL RESEARCH LETTERS, VOL. 34, L08701, doi:10.1029/2006GL029022, 2007

Click Here for Full Article

Assessing consistency between EOS MLS and ECMWF analyzed and forecast estimates of cloud ice

J.-L. Li,[1] J. H. Jiang,[1] D. E. Waliser,[1] and A. M. Tompkins[2]

Received 7 December 2006; accepted 14 March 2007; published 17 April 2007.

[1] Cloud ice water content (IWC) from MLS retrievals and ECMWF analyses and forecasts are compared for August 2004 to July 2005. ECMWF data are sampled along MLS tracks and filtered according to MLS sensitivity. At 147 hPa, there is good spatial agreement with the analyses biased high by 10%. Over landmasses, the analyses are biased low up to 50%. This underestimation grows in the forecasts, with a 40% reduction by day 10. At 215 hPa, the analyses are biased low by 10–60%. However, at this level the forecast IWC undergoes little change. These biases, in conjunction with those in precipitation and top of the atmosphere radiative fluxes, along with consideration of the changes in vertical velocity, cumulus cloud mass flux and cloud top detrainment, indicates a systematic reduction of the modeled deep convection over the warm pool in conjunction with a weakened large-scale circulation and enhanced upper-level vertical stratification. **Citation:** Li, J.-L., J. H. Jiang, D. E. Waliser, and A. M. Tompkins (2007), Assessing consistency between EOS MLS and ECMWF analyzed and forecast estimates of cloud ice, *Geophys. Res. Lett.*, *34*, L08701, doi:10.1029/2006GL029022.

1. Introduction

[2] Upper–tropospheric (UT) ice clouds can strongly influence global climate through their effects on the radiation budget of the earth and the atmosphere [e.g., *Starr and Cox*, 1985; *Liou*, 1986; *Ramanathan et al.*, 1989; *Stephens*, 2005]. In addition, they play a very important role in determining the spatial structure of precipitation, the vertical structure of latent heating and the time scale of the atmospheric hydrological cycle [e.g., *Webster*, 1994]. Although observations of ice clouds have been made using satellites [e.g., *Rossow and Garder*, 1993] as well as in situ methods [e.g., *McFarquhar et al.*, 1999], our understanding of UT cloud processes, particularly their microphysical makeup and vertical distribution, remains limited. Even basic quantities such as ice water content (IWC) have been difficult to characterize from space due to penetration and sensitivity shortcomings in the visible and infrared wavelengths and nadir-viewing geometry.

[3] The EOS MLS on the Aura satellite platform provides global observations of cloud IWC profiles. These observations offer a new opportunity to study UT cloud processes in global atmospheric models, such as the integrated forecast system (IFS) of the European Centre for Medium Range Weather Forecasts (ECMWF). *Li et al.* [2005] provided an initial assessment of the ECMWF model analyses (in addition to other global climate models) in representing global UT IWC, using one month of the MLS IWC measurements from January 2005. They found that the spatial agreement between MLS and ECMWF were quite good, although the MLS estimates were generally higher by a factor of 2–3 than the ECMWF fields, particularly over tropical landmasses. Some of the inconsistencies between the analyses and satellite values might have arisen from sampling differences (e.g., diurnal cycle), instrument sensitivity and precision, and/or systematic biases in the retrievals and/or analyses.

[4] This study aims to improve the preliminary study of *Li et al.* [2005] by extending the study period to an entire year of overlapping observations and model output, by explicitly accounting for the MLS algorithm/instrument sensitivity in the comparisons, and by sampling the ECMWF analyses only at the times and locations of the MLS retrievals. In addition, in order to better understand the nature and impact of the systematic biases in the ECMWF model, the ECWMF forecasts are also investigated.

2. Data

2.1. MLS Satellite Observations

[5] The MLS onboard the Aura satellite, operational since August 2004, has five radiometers measuring microwave emissions from the Earth's atmosphere in a limb-scanning configuration to retrieve chemical composition, water vapor, temperature and cloud ice. The retrieved parameters consist of vertical profiles on fixed pressure surfaces having near-global (82°N–82°S) coverage. The MLS IWCs are derived from cloud-induced radiances (CIR) using modeled CIR-IWC relations based on the MLS 240 GHz measurements. The IWCs at 147 and 215 hPa have a vertical resolution of ~3.5 km and a horizontal along-track resolution of ~160 km for a single MLS measurement along an orbital track. This study uses MLS version 1.51 IWCs [*Livesey et al.*, 2005], similar to IWCs discussed by *Li et al.* [2005]. In this version, the estimated precision for the IWC measurements is approximately 0.4, 1.0 and 4.0 (mg m^{-3}) at 100, 147, and 215 hPa, respectively, which account for combined instrument plus algorithm uncertainties associated with a single observation. In this study we focus on the 215 hPa and 147 hPa levels. The data used in this study are from the period August 2004 to July 2005. It is important to note that the MLS IWC data has yet to be comprehensively validated. A detailed description and validation of the MLS IWC retrieval is given by *Wu et al.* [2006] (D. L. Wu et al., Aura MLS cloud ice measurements and comparisons with CloudSat and other

[1]Jet Propulsion Laboratory, Pasadena, California, USA.
[2]European Centre for Medium-Range Weather Forecasts, Reading, UK.

Copyright 2007 by the American Geophysical Union.
0094-8276/07/2006GL029022$05.00

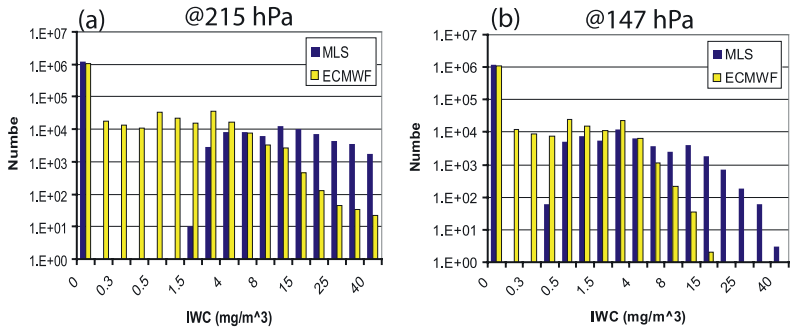

Figure 1. Histogram of ice water content (mg m^{-3}) in August 2004∼July 2005 for MLS (dark blue) and sampled ECMWF (yellow) at (a) 215 hPa and (b) 147 hPa.

correlative data, submitted to *Journal of Geophysical Research*, 2007).

[6] Shown in Figure S1 of the auxiliary material,[1] Figure S1a illustrates the MLS IWC retrievals at 147 hPa for January 2nd 2005 with individual measurement locations shown as small black dots and non-zero IWC values shown as colored dots. Note that the Aura satellite has equatorial crossing times of approximately 01:30 LST and 13:30 LST. The daily and annual (August 2004 to July 2005) means shown in Figure S1b are computed from the total IWC amounts divided by the total number of measurements (including cloud free conditions) and binned onto a $4° \times 8°$ latitude-longitude grid. Figure S1b reveals several areas of deep convective activity over the W. Pacific, Central Equatorial Pacific and Indian Oceans with high IWC values of 2–4 mg m^{-3}. Figure S1a shows a series of large IWC values over S. America (see track denoted with an A) with IWC values up to 10–12 mg m^{-3}. Upon averaging to the $4° \times 8°$ grid, the IWC values in this region drops to about 4 mg m^{-3} (Figure S1b).

2.2. ECMWF Analyses and Forecasts

[7] The daily analysis values of IWC at 00, 06, 12 and 18Z during August 2004 to July 2005 from the ECMWF Integrated Forecast System (IFS) are used. The data assimilation system (DAS) uses a four dimensional variational analysis approach with a 12 hour assimilation window [*Rabier et al.*, 1998]. This employs simplified physics in the tangent linear model [*Mahfouf*, 1999; *Janiskova et al.*, 2002], which for cloud processes is based on a simple saturation adjustment scheme combined with the cloud scheme of *Slingo* [1987]. The final analysis is derived from a short forecast using the full nonlinear forecast model which uses a cloud scheme based on that of *Tiedtke* [1993], and modified by *Jakob* [2000]. The scheme introduces prognostic equations for cloud cover and cloud water content, which is diagnostically divided into liquid and ice according to temperature. An important aspect of the scheme is its link to other processes which provide sources and sinks of the cloud variables, one of the most important being detrainment from the mass-flux deep convection parameterization.

[8] It should be noted that no cloud affected radiances or brightness temperature are currently assimilated from remotely-sensed platforms (see *Chevallier et al.* [2004] for details) although recently microwave information in rainy regions have been utilized for the first time [*Bauer et al.*, 2002]. This implies that the cloud properties in the analysis are a direct result of the analyzed temperature, humidity and velocity fields, and also the physics of the cloud scheme. The MLS data are not assimilated in the ECMWF DAS, and thus the MLS IWC retrievals can be considered an independent validation dataset. To examine how the forecast model systematic bias evolves when unconstrained by data, IWC from the model forecast ranges of 03, 12, 24, 48, 120 and 240 hours at 215 hPa and above during August 2004 to July 2005 are examined. To account for differences in spatial resolution, the ECMWF data were re-gridded to the $4° \times 8°$ MLS latitude-longitude grid.

3. Results

3.1. Sampling Methodology

[9] To account for differences between MLS and ECMWF sampling characteristics (MLS twice daily at the same local times vs. four synoptic times per day for ECMWF), we sample the ECMWF data along the MLS orbit tracks. This sampling is based on a distance-weighted linear average from the two nearest grid points considering the latitude, longitude, vertical and temporal dimensions. This procedure gives an ECMWF IWC value for each value retrieved by MLS (hereafter referred to as "sampled" values). We have examined and compared a number of daily MLS and sampled ECMWF IWC maps (e.g., Figure S1d), and found that the two data sets are in relatively good agreement, particularly in terms of geographical distribution over the oceans. In general, the sampled ECMWF IWC values are smaller than the MLS estimates. In addition, over tropical and mid-latitude landmasses, greater disagreement is typically found between the sampled ECMWF values and the MLS data. The maps in Figure S1 provide an illustrative example. Figure S1b shows the daily gridded values from MLS for January 2nd 2005. Figure S1c shows the gridded ECMWF values using all the data from January 2nd while Figure S1d shows the gridded sampled ECMWF values. It is evident that sampling the ECMWF data along the orbit track provides for more consistent agreement between the two sets of data. The locations of the IWC maxima are generally well captured by the sampled ECMWF values over oceans, particularly over Western Pacific.

[1]Auxiliary materials are available in the HTML. doi:10.1029/2006GL029022.

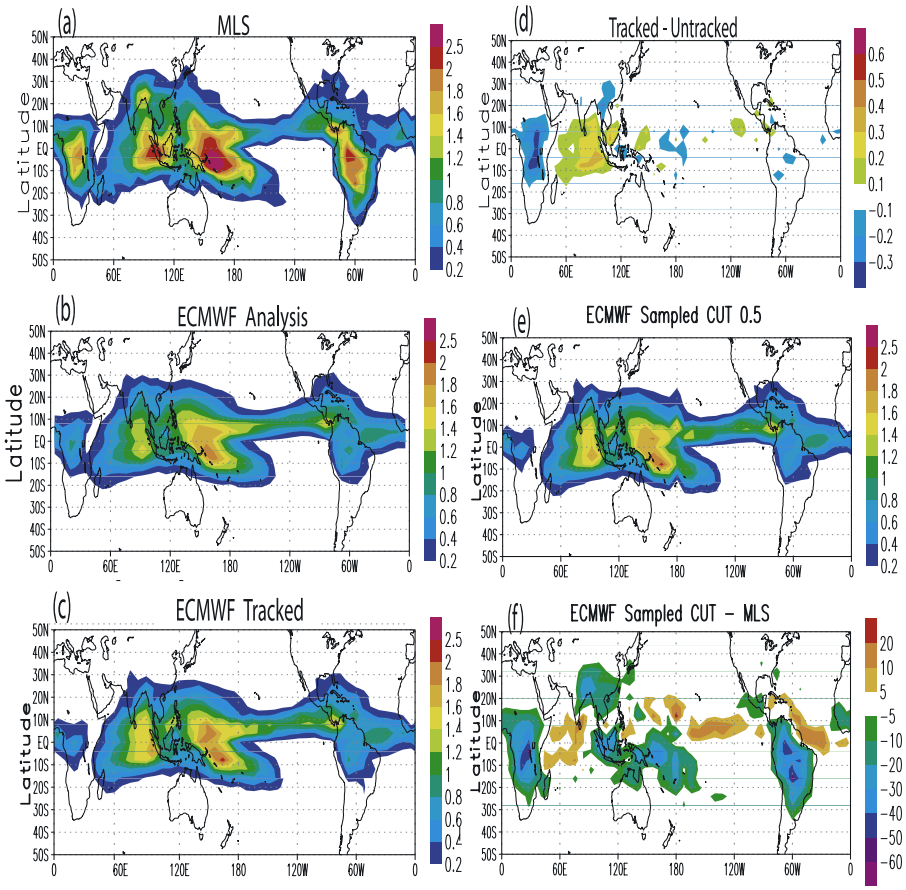

Figure 2. Maps of annual average ice water content (mg m^{-3}) for period of August 2005∼July 2005 mean at 147 hPa from (a) the EOS MLS, (b) the ECMWF analyses, (c) the ECMWF analyses sampled along the MLS tracks, (d) the difference after sampling applied on the ECMWF analyses, (e) the same as Figure 2c but with MLS cutoff values applied, and (f) the difference between Figures 2e and 2a (%) relative to MLS.

[10] The sensitivity limitations of the MLS instrument/retrievals are examined by comparing the probability distribution functions (PDFs) of the MLS and ECMWF IWC values (Figure 1). The sampled ECMWF values have fewer high IWC values than MLS data at both levels. Moreover, the PDFs clearly illustrate the sensitivity limits of the MLS instrument, namely that the precision of the MLS retrievals dictates a lower limit on the IWC values that can be obtained; roughly ∼1.5 (mg m^{-3}) at 215 hPa and ∼0.5 (mg m^{-3}) at 147 hPa. In order to account for this sensitivity limit in the comparisons described below, these lower limits are applied to the sampled ECMWF values. That is, any sampled ECMWF IWC value less than 1.5 (mg m^{-3}) at 215 hPa and less than 0.5 (mg m^{-3}) at 147 hPa is set to zero which is equivalent to what happens in the MLS retrieval. These values are referred to as filtered values.

3.2. ECMWF Analyses

[11] A comparison of the annual mean values from MLS (Figure 2a) and unfiltered ECMWF values (Figure 2b) at 147 hPa shows good agreement over most tropical regions in terms of spatial distribution. The disagreement in terms of magnitude, on the other hand, are illustrated by the peak values over S. America, Central Africa, eastern Indian Oceans and the western Pacific which tend to be higher in the MLS estimates than the ECMWF values by a factor of 2–4. Over the Eastern Pacific and Atlantic ITCZs, the MLS values are slightly lower than ECMWF values. Figure 2c shows the annual ECMWF IWC sampled along the MLS orbital tracks, and Figure 2d shows the difference between the sampled and unsampled ECMWF values. The main impacts of the sampling were to decrease the values over central Africa and increase them slightly over the parts of the central and eastern Indian Ocean. Given that high cloudiness and convection as "measured" by OLR indicate late afternoon maxima over tropical landmasses [*Lin et al.*, 2000; *Lin et al.*, 2002; *Tian et al.*, 2004], it is reasonable that the sampled ECMWF IWC would decrease given the 1:30 LST (descending orbit) and 13:30 LST (ascending orbit) equatorial sampling times miss the maxima. However, it isn't then clear why such a difference doesn't also occur over S. America. This may be related to the known shortcomings in the representation of the diurnal cycle over S. America within the ECMWF model [*Betts and Jakob*, 2002]. In a similar manner, given the rather weak observed diurnal cycle over the ocean regions, it is not obvious why such an impact would be exhibited over the oceans, and then only the Indian Ocean. Additional study on the diurnal cycle in the observations and the ECMWF analyses are required to fully understand the reasons for these impacts from the sampling.

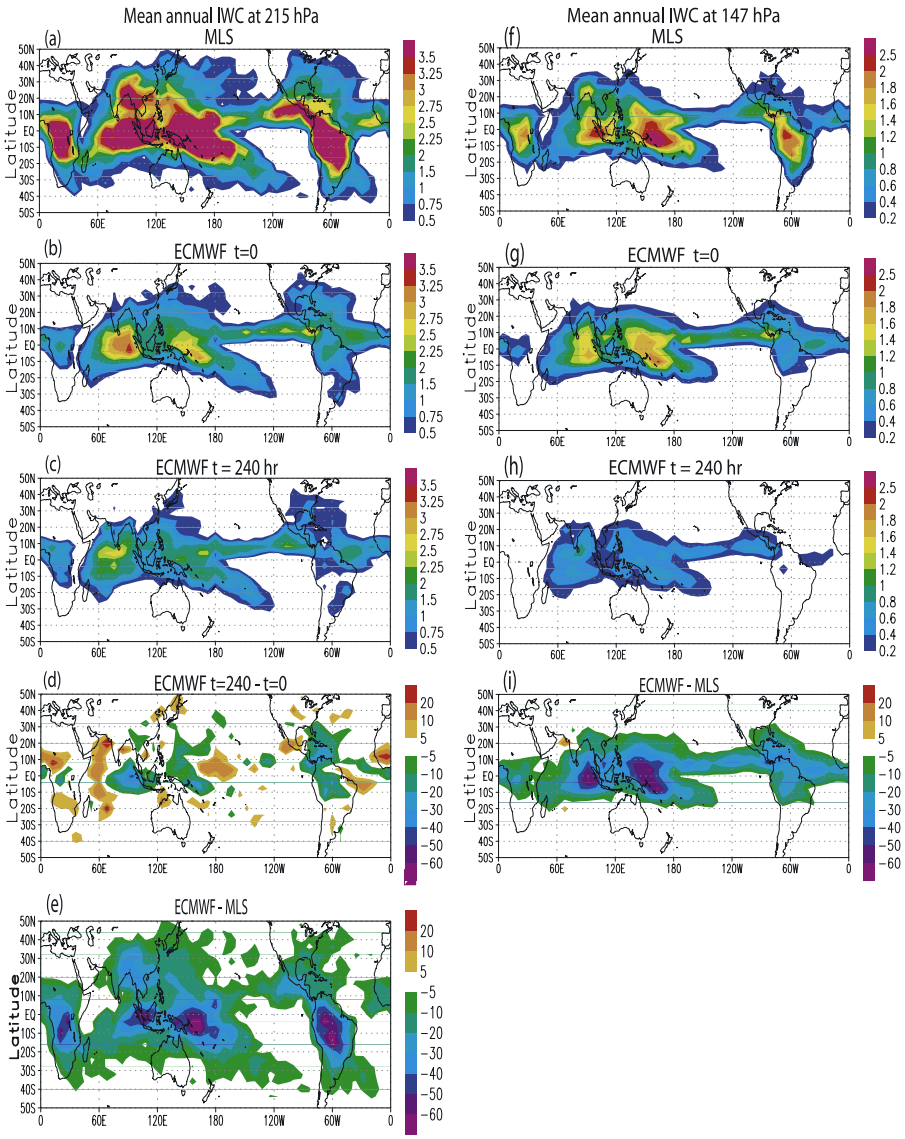

Figure 3. Maps of mean annual ice water content (mg m^{-3}) at 215 hPa based on (a) MLS, (b) ECMWF initial time, (c) day-10 ECMWF forecast, (d) the difference between Figures 3c and 3b, and (e) the difference between Figures 3b and 3a w.r.t. MLS (%). Maps of mean annual ice water content (mg m^{-3}) at 147 hPa based on (f) MLS, (g) ECMWF initial time, (h) day-10 ECMWF forecast, and (i) the difference between Figures 3h and 3g.

[12] When the MLS sensitivity cutoff is considered, small values of ECMWF IWC are set to zero, and thus the mean values are slightly reduced as is evident when comparing Figure 2c and the filtered data in Figure 2e. This of course tends to slightly enhance (~5%) the disagreement in magnitude found between the sampled ECMWF and the MLS IWC values discussed above. Examination of the difference between the sampled/filtered ECMWF data and the MLS retrievals (Figure 2f) shows that ECMWF IWC values are less than MLS values by about 30~50% relative to MLS over nearly all the tropical landmasses as well as over much of the South Pacific Convergence Zone (SPCZ). Similar results to these are found for other levels examined. The ECMWF IWC values are slightly greater (~10%) than the MLS values over most tropical oceanic regions, with the ITCZ regions in the Eastern Pacific and Atlantic ITCZs being especially prominent.

3.3. ECMWF Forecast

[13] The evolution of the model's systematic bias is examined during the 10 day forecast range. In this case, the forecast values were sampled along the MLS orbital tracks and filtered as described above for the analysis values. Figure 3 shows mean annual IWC maps from the MLS, ECMWF analyses, and ECMWF at a lead time of 10 days for 215 hPa and 147 hPa. For the 215 hPa level (and below, not shown), the IWC geographical distributions and quantitative values from both the analyses (Figure 3b) and day-10 forecasts (Figure 3c) exhibit differences of about 20% or less relative to the initial time (Figure 3b), and thus the day-10 forecast differences with MLS IWC (Figure 3a) are consistent with the discussion above. For the 147 hPa level, on the other hand, there is a rather large systematic bias that develops with smaller IWC values for the day-10 forecast (Figure 3h), with reductions ranging from about

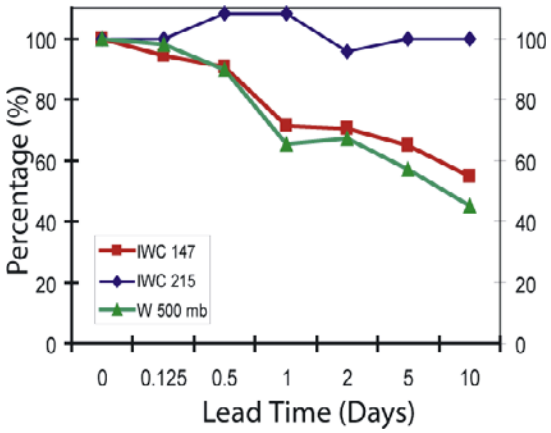

Figure 4. The percentage (respect to initial time) of global mean IWC forecast evolutions from initial hour to day-10 forecast for 215 hPa (dark blue line) and 147 hPa (red line). Percentage (respect to initial time) of mean vertical velocity (green line) in the west tropical Pacific area (10°S–10°N; 70°E–170°E) at 500 hPa.

10–20% over most tropical regions and exceeding 50% in the warm pool regions of the Western Pacific and Indian Oceans (Figure 3i).

[14] In terms of the forecast evolution (Figure 4), there is no change at 215 hPa and a 50% reduction at 147 hPa in the tropical mean (30N–30S) IWC by day 10. These values indicate a rapidly developing and larger systematic bias at the 147 hPa level and above, and when considered in conjunction with the spatial structures of the biases suggest a change in the structure of the large-scale circulation. Inspecting the mean vertical velocity at 500 hPa in the ascending branch of the Walker Circulation (10S–10N; 70E–170E) illustrates a decrease strength of the tropical circulation of about 50% by day 10 (green line with triangles). In other words, these systematic IWC forecast biases appear to be associated with a weakening of convection and circulation as the model forecast evolves. Given the significant changes that occur in the first 24 hours of the forecast indicates biases that are likely introduced by fast processes such as parameterized moist convection.

[15] Comparing the day 10 top-of-atmosphere net infrared (IR) fluxes and the precipitation fields to Clouds and the Earth's Radiant Energy System (CERES) [e.g., *Wielicki et al.*, 1998] and Global Precipitation Climatology Project (GPCP, V2; *Adler et al.* [2003]) datasets, respectively, provides further evidence of the relative lack of deep convective activity in these regions. The auxiliary material Figure S4 shows that in terms of IR, there is a strong negative bias over all three tropical regions of America, Africa and the Maritime continent, in agreement with the MLS maps. This bias is consistent with one or more of the following model deficiencies: lack of deep convective activity, too much ice sedimentation (or an equivalent sink mechanism) that reduces anvil ice contents, too low convective detrainment levels or too small anvil cloud coverage. The MLS data indicates that ice is lacking and thus it is likely to be one or both of the first two causes. The negative precipitation biases over America and the Maritime continent indicates that a lack of deep convection is present in these two regions. However, the fact that the reduction occurs at 147 hPa and not below also indicates that the convection is detraining at a lower level as the forecast progresses. The lack of significant biases of cloud cover to International Satellite Cloud Climatology Project (ISCCP) data, and shortwave fluxes compared to CERES data (not shown), appears to corroborate these conclusions. It should be emphasized that errors such as too-low detrainment level of deep convection are not necessarily due to shortcomings in the convection scheme itself, but can be due to other model components altering the upper tropospheric stability as the forecast progresses (not shown).

4. Summary and Discussion

[16] IWC estimates from the MLS for the period August 2004 to July 2005 are compared to both ECMWF analyses and forecasts. The ECMWF IWC is sampled along MLS orbit tracks and assigned zero values when it is less than the lower sensitivity limit of the MLS instrument. The impact of both of these sampling procedures is described and illustrated.

[17] The results of the comparison between the MLS and sampled ECMWF analyzed IWC show that for the annual mean, the overall geographical distribution agrees quite well. Over the oceans the ECMWF analyses are larger than MLS values by about 10% but over tropical landmass and maritime continent, the ECMWF analyses are smaller than the MLS IWC by up to 50%. For 215 hPa, the MLS IWCs are higher than ECMWF values globally, with differences ranging up to 60% relative to MLS (Figure 3e).

[18] The ECMWF forecasts were examined at lead times ranging from 3 to 240 hours. At 215 hPa, the global (or tropical) average IWC shows no obvious systematic change although the IWC values tend to decrease over the tropical land masses including a large region associated with the Maritime Continent/Indo-Pacific Warm pool and generally increase over other convective areas of the tropical oceans. Spatially, these changes in IWC bear some similarity to the biases between MLS estimates and the sampled ECMWF analyzed values. At 147 hPa, the changes with forecast lead time are even starker, with a significant reduction (up to 60%) in IWC found across the global tropics by day 10, in particular over the Indo-Pacific warm pool region.

[19] Examination of the mid-tropospheric vertical velocity shows a systematic decrease (~50%) in the large-scale upward vertical velocity over this same region. To obtain a more quantitative picture of the interactions between the dynamics, thermodynamics and hydrology in the upper troposphere, a 10-day forecast with additional tendency diagnostics was conducted, producing time series of area-average cloud ice detrainment, cumulus cloud mass flux and vertical stratification over this same region at 316, 215 and 147 hPa. These revealed that, as the vertical velocity and IWC at 147 hPa decreases, there are concurrent reductions in cloud ice detrainment (Figure S2) and cumulus cloud mass flux (Figure S3) at all three levels. The cumulus cloud mass flux decreases are, however, larger at 147 hPa (~50% left at day 10) than at the other two levels (~75% left at day 10). Additionally, the large-scale stratification increases between 500 and 147 hPa over the forecast period (not shown). The implication is that the spatial structure of the

forecast biases is influenced by the evolution of the large-scale circulation and/or in part by the strength of model convection. Further examination of the temporal evolution of these lead-time dependent biases shows that about half of the systematic reduction in IWC occurs in the first 24 hours. These characteristics in the development of the forecast biases, with a fast adjustment occurring over the first day, along with supporting evidence from outgoing longwave, precipitation and cloud cover comparisons, indicate too little convective activity and thus possible shortcomings in the parameterizations of moist physical processes of clouds and convection, which impact the large-scale circulation. These suggest that the decrease of IWC at 147 hPa might be in part associated with the interplay and feedback between the upper level stratification, the cloud ice detrainment level and convective activity.

[20] These first global measurements of height-resolved ice water content thus permit the model community to better guide and constrain the formulation of convective and cloud processes in atmospheric models. At present there are still considerable uncertainties and limitations regarding the MLS IWC retrievals, most notably coarse vertical resolution, the limitation in scope to the upper troposphere, and as yet a lack of adequate independent validation. It is expected that the recently launched CloudSat mission [*Stephens et al.*, 2002] will rectify or improve some of these shortcomings, especially by providing increased vertical resolution as well as a complimentary retrieval technology (i.e. nadir-viewing cloud radar). It is hoped that future missions can provide improved sampling capabilities, particularly greater horizontal coverage and a better representation of the diurnal cycle (both MLS and CloudSat only sample along a single ground track and at the same two local times per day). These recent NASA missions as well as, hopefully, future missions with improved capabilities, can be expected to lead to significant improvements in our understanding, as well as our simulation and prediction capabilities, of cloud-related processes.

[21] **Acknowledgments.** Support was provided by JPL's RTD (first author) and HRD Funds (third author), and the NASA MAP Program. We are grateful to Michael Schwartz, J. Waters, and JPL's MLS team. This work was performed at the JPL/Caltech under contract with NASA.

References

Adler, R. F., et al. (2003), The Version 2 Global Precipitation Climatology Project (GPCP) monthly precipitation analysis (1979–Present), *J. Hydrometeorol.*, *4*, 1147–1167.

Bauer, P., G. Kelly, and E. Andersson (2002), SSM/I radiance assimilation at ECMWF, paper presented at ECMWF/GEWEX Workshop, Reading, U.K., 8–11 July.

Betts, A. K., and C. Jakob (2002), Evaluation of the diurnal cycle of precipitation, surface thermodynamics, and surface fluxes in the ECMWF model using LBA data, *J. Geophys. Res.*, *107*(D20), 8045, doi:10.1029/2001JD000427.

Chevallier, F., P. Lopez, A. M. Tompkins, M. Janisková, and E. Moreau (2004), The capability of 4D-Var systems to assimilate cloud-affected satellite infrared radiances, *Q. J. R. Meteorol. Soc.*, *130*, 917–932.

Jakob, C. (2000), The evaluation of cloud parameterizations in GCMs: Are we doing the best we can?, paper presented at ECMWF/EuroTRMM Workshop on Assimilation of Clouds and Precipitation, Reading, U.K., 6–9 Nov.

Janiskova, M., J. F. Mahfouf, J.-J. Morcrette, and F. Chevallier (2002), Linearized radiation and cloud schemes in the ECMWF model: Development and evaluation, *Q. J. R. Meteorol. Soc.*, *128*, 1505–1527.

Li, J.-L., et al. (2005), Comparisons of EOS MLS cloud ice measurements with ECMWF analyses and GCM simulations: Initial results, *Geophys. Res. Lett.*, *32*, L18710, doi:10.1029/2005GL023788.

Lin, X., D. A. Randall, and L. D. Fowler (2000), Diurnal variability of the hydrological cycle and radiative fluxes: Comparison between observations and a GCM, *J. Clim.*, *13*(23), 4159–4179.

Lin, X., L. D. Fowler, and D. A. Randall (2002), Flying the TRMM satellite in a general circulation model, *J. Geophys. Res.*, *107*(D16), 4281, doi:10.1029/2001JD000619.

Liou, K.-N. (1986), Influence of cirrus clouds on weather and climate processes: A global perspective, *Mon. Weather Rev.*, *114*, 1167–1199.

Livesey, N. J., et al. (2005), Version 1.5 Level 2 data quality and description document, *JPL Document D-32381*, Pasadena, Calif.

Mahfouf, J.-F. (1999), Influence of physical processes on the tangent-linear approximation, *Tellus, Ser. A*, *51*, 147–166.

McFarquhar, G. M., A. J. Heymsfield, A. Macke, J. Iaquinta, and S. M. Aulenbach (1999), Use of observed ice crystal sizes and shapes to calculate mean-scattering properties and multi-spectral radiances: CEPEX April 4, 1993, case study, *J. Geophys. Res.*, *104*, 31,763–31,779.

Rabier, F., J.-N. Thepaut, and P. Courtier (1998), Extended assimilation and forecast experiments with a four-dimensional variational assimilation, *Q. J. R. Meteorol. Soc.*, *124*, 1861–1887.

Ramanathan, V., et al. (1989), Cloud-radiative forcing and climate: Results from the Earth Radiation Budget Experiment, *Science*, *243*, 57–63.

Rossow, W. B., and L. C. Garder (1993), Validation of ISCCP cloud detection, *J. Clim.*, *6*, 2370–2393.

Slingo, J. (1987), The development and verification of a cloud prediction scheme for the ECMWF model, *Q. J. R. Meteorol. Soc.*, *113*, 899–927.

Starr, D. O., and S. K. Cox (1985), Cirrus clouds. part II: Numerical experiments on the formation and maintenance of cirrus, *J. Atmos. Sci.*, *42*, 2682–2694.

Stephens, G. L. (2005), Cloud feedbacks in the climate system: A critical review, *J. Clim.*, *18*, 237–273.

Stephens, G. L., et al. (2002), The CloudSat mission and the A-Train: A new dimension of space-based observations of clouds and precipitation, *Bull. Am. Meteorol. Soc.*, *83*, 1771–1790.

Tian, B., B. J. Soden, and X. Wu (2004), Diurnal cycle of convection, clouds, and water vapor in the tropical upper troposphere: Satellites versus a general circulation model, *J. Geophys. Res.*, *109*, D10101, doi:10.1029/2003JD004117.

Tiedtke, M. (1993), Representation of clouds in large-scale models, *Mon. Weather Rev.*, *121*, 3030–3061.

Webster, P. J. (1994), The role of hydrological processes in ocean-atmosphere interactions, *Rev. Geophys.*, *32*, 427–476.

Wielicki, B. A., et al. (1998), Clouds and the Earth's Radiant Energy System (CERES) algorithm overview, *IEEE Trans. Geosci. Remote Sens.*, *36*, 1127–1141.

Wu, D. L., J. H. Jiang, and C. P. Davis (2006), EOS MLS cloud ice measurements and cloudy-sky radiative transfer model, *IEEE Trans. Geosci. Remote Sens.*, *44*, 1156–1165.

J. H. Jiang, J.-L. Li, and D. E. Waliser, Jet Propulsion Laboratory, MS 183-601, 4800 Oak Grove Drive, Pasadena, CA 91109, USA. (jli@jpl.nasa.gov)

A. M. Tompkins, European Centre for Medium-Range Weather Forecasts, Shinfield Park, Reading RG1 1NT, UK.